

SHED: Style-Homogenized Embedding Alignment for Domain Generalization

Kai Gan Tong Wei*

¹School of Computer Science and Engineering, Southeast University, Nanjing 210096, China

²Key Laboratory of Computer Network and Information Integration (Southeast University),

Ministry of Education, China

{gank, weit}@seu.edu.cn

Abstract

Domain generalization aims to enhance model robustness against unseen domains with embedding distribution shifts. While large-scale vision-language models like CLIP exhibit strong generalization, their direct image-text embedding alignment suffers from inherent information asymmetry: images encode both class semantics and domain-specific styles, whereas text prompts primarily convey basic class cues. This asymmetry hinders generalization to novel domains in realistic scenarios. To address this, we propose Style-Homogenized Embedding alignment for Domain-generalization (SHED), a novel CLIP-based method that aligns style-homogenized embeddings instead of raw representations from encoders in CLIP. During training, SHED removes domain-specific style centroids from both image embeddings computed per source domains and text embeddings which are averaged across diverse prompt templates and stripped of a global centroid. For inference, considering the lack of target domain information, SHED projects diverse textual domain centroids into the visual space and aggregates predictions via membership weighting. Extensive experiments on five benchmarks show SHED achieves state-of-the-art performance, outperforming prior methods significantly (e.g., +4.0% on DomainNet vs. standard fine-tuning).

1 Introduction

When machine learning models are deployed in real-world open environments, they inevitably encounter samples from unseen domains with embedding distribution shifts. To improve generalization to unseen domains, domain generalization methods Zhou *et al.* [2022a]; Li *et al.* [2018a,b] aim to learn domain-invariant embeddings by leveraging knowledge from source domains and maintaining robustness across diverse unknown domains. However, models trained from scratch on small-scale datasets often struggle to exhibit strong generalization capabilities across various domains.

Fortunately, recent advances such as CLIP Radford *et al.* [2021], which is trained on large-scale image-text pairs, have achieved notable success in numerous downstream tasks Li *et al.* [2021]; Zhou *et al.* [2022c,b]; Wu *et al.* [2023]; Gan and Wei [2024] due to its rich semantic representation and robust zero-shot learning ability. Nevertheless, current mainstream methods predominantly emphasize adaptation to specific domains Lai *et al.* [2023]; Feng *et al.* [2024], which can significantly impair their generalization capability to unseen style domains. To address this challenge, CLIPood Shu *et al.* [2023] introduced margin metric softmax and beta moving average to preserve the original semantic associations of pre-trained CLIP. CLIPCEIL Yu *et al.* [2024] refined the embedding channels in the visual domain to ensure they contain domain-invariant and class-relevant embeddings by using a lightweight adapter. However, a key limitation of existing methods is their reliance on direct alignment between images embeddings and manually designed class template texts embeddings. Since images encode both class and domain style information while the texts contain only basic class cues, this asymmetric alignment impairs the model’s generalization ability to unseen domains. Domain-specific attributes (e.g., artistic style in paintings) may dominate image representations, causing spurious correlations with text centroids and misleading predictions. Specifically, as illustrated in Figure 2a, we observe that in the original CLIP embedding space, each image centroid exhibits high similarity with multiple class text centroids, which makes it difficult to infer the true class during inference accurately. This naturally raises the question: *Can we achieve symmetric alignment training between images and text embeddings?*

In this paper, we propose a novel CLIP-based domain generalization method SHED to answer this question. Instead of aligning the raw image-text embeddings directly, SHED aligns the embeddings after removing domain-specific style information. As visualized in Figure 1, SHED exploits a key geometric insight: embeddings across various domains and template-based texts share a latent structural consistency where samples from the same class consistently point in similar directions relative to their respective domain or text centroids. This structure consistency motivates us to explicitly performing style-homogenized embedding alignment within this shared geometric structure. Concretely, for images, we derive style-homogenized image embeddings by first com-

*Corresponding author

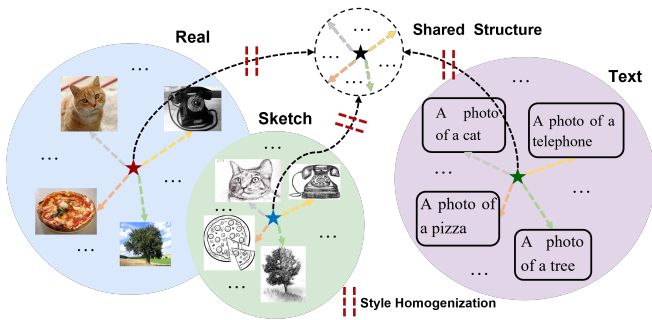


Figure 1: An illustration of the embedding space distribution for image samples from different domains and class texts constructed using templates. The red dashed line indicates the gap between the image and text modalities.

puting the centroid of each domain, and then subtracting it from the corresponding sample embeddings. For texts, we generate text embeddings using various templates and average them to derive a representative text embedding for each class. We then calculate a global text centroid across all classes and subtract it from each class embedding to obtain style-homogenized text embeddings. As shown in Figures 2a and 2b, the style-homogenized image and text embeddings exhibit more discriminative inter-class separability compared to the original CLIP embeddings, which facilitates more accurate and robust classification Shi *et al.* [2024] across different domains. Unsurprisingly, when using style-homogenized image and text embeddings to calculate zero-shot style-homogenized probability, we find it consistently achieve superior zero-shot classification performance across various domains compared to using original CLIP embeddings in Figure 3.

During inference, it is challenging to obtain style-homogenized image embeddings due to the domain identity of images are unavailable. To tackle this issue, we manually construct multiple textual domain centroids and project them into the visual space to approximate potential image domain centroids. Accordingly, we compute the membership degree of the test samples to each visual centroid, which serves as weights for aggregating the style-homogenized probabilities from these centroids. As a result, SHED eliminates dependence on ground-truth domain centroids and can predict style-homogenized probabilities for arbitrary samples.

Our main contributions can be summarized as follows:

- We propose SHED, a novel domain generalization framework that enhances prediction on unseen domains. It uniquely addresses the inherent information asymmetry in CLIP by aligning style-homogenized embeddings, rather than performing direct alignment on raw visual and textual representations.
- We propose the aggregation of multiple centroids predictions to equip the model with the capability to handle samples from any target domains during inference.
- Extensive experimental analyses show that SHED achieves state-of-the-art performance on multiple

benchmarks across various domains, e.g., SHED improves ERM by over 4.0% on DomainNet.

2 Related Work

Vision-Language Models Recently, vision-language pre-training Radford *et al.* [2021]; Jia *et al.* [2021]; Li *et al.* [2022, 2023]; Pham *et al.* [2023]; Luo *et al.* [2025]; Gan *et al.* [2025]; Wei *et al.* [2026, 2024] have demonstrated remarkable success in various downstream tasks through fine-tuning. Specifically, CLIP Radford *et al.* [2021] leverages contrastive learning on a large collection of image-text pairs to learn semantic associations between visual and textual modalities, enabling cross-modal retrieval and classification. BLIP Li *et al.* [2022] integrates vision-language matching and generation tasks with guided objectives to enhance image-text alignment, enabling strong performance on both vision-language understanding and generation tasks. BLIP-2 Li *et al.* [2023] introduces a lightweight query transformer between the vision encoder and the language model to facilitate efficient image-text alignment. Additional, vision-language models can achieve significant performance improvements on downstream tasks through various fine-tuning strategies Houlsby *et al.* [2019]; Chen *et al.* [2022]; Jia *et al.* [2022], including long-tailed learning Dong *et al.* [2022]; Shi *et al.* [2024], test-time adaptation Zhou *et al.* [2023]; Osowiecki *et al.* [2024] and domain generalization Shu *et al.* [2023]; Yu *et al.* [2024]. To address the challenge of domain generalization, we investigate how CLIP’s robust vision-language pre-training can be adapted to enhance model robustness across unseen domains.

Domain Generalization The goal of domain generalization is to train models on data from multiple known domains, while evaluating them on data from entirely unseen domains. Specifically, SagNets Nam *et al.* [2021] improve generalization and adaptability in cross-domain tasks by disentangling style and category representations, thereby reducing the CNN’s reliance on style-biased embeddings. BNE Segu *et al.* [2023] employs domain-specific batch normalization layers to extract domain-dependent embeddings and models each domain in a shared latent space based on distance. mDSDI Bui *et al.* [2021] operates by decomposing latent embeddings into domain-invariant and domain-specific components. It jointly learns representations and employs meta-learning to optimize the domain-specific part. However, existing methods primarily rely on direct alignment of image and text embeddings, neglecting the inherent information asymmetry between the two modalities. In contrast, our work is the first to systematically address this asymmetry by proposing a symmetric alignment of style-homogenized embeddings.

Domain Generalization via CLIP Considering the strong semantic generalization capabilities of vision-language models such as CLIP, recent studies have begun to explore how to leverage CLIP to improve performance on domain generalization tasks. MIRO Cha *et al.* [2022] introduces a pre-trained model as an approximation to the oracle model and maximizes the mutual information with it to encourage the learning of more generalizable representations. VL2V-ADiP Addepalli *et al.* [2024] enhances the generalization ability

of the student model by aligning the visual and language modalities of the teacher VLM with the visual modality of the student, followed by distillation of the aligned representations, while preserving the student’s pretrained characteristics. CLIPood Shu *et al.* [2023] introduces a Margin Metric Softmax loss with class-adaptive boundaries to fine-tune the model by leveraging semantic relationships in the text modality, while employing a Beta distribution-based moving average to fuse the pretrained zero-shot model and the fine-tuned model. However, existing methods primarily rely on direct alignment of image and text embeddings, neglecting the inherent information asymmetry between the two modalities.

3 The Proposed Method

In this section, we provide a detailed description of SHED which includes style-homogenized alignment during model training and domain-agnostic centroid aggregation for unknown domain sample inference.

3.1 Preliminaries

In this paper, we investigate the problem of domain generalization. Formally, our objective is to train the model on the source training set $\{\mathcal{D}^s = \{(x_i^s, y_i^s)\}_{i=1}^{n_s}\}_{s=1}^S$, where S represents the number of domains and n_s denotes the number of samples in each source domain. $y_i^s \in \{0, 1\}^C$ is the ground truth class label of C -class classification task for image x_i^s . During the testing phase, we evaluate the model on a novel domain dataset $\mathcal{D}^{\text{test}} = \{x_j\}_{j=1}^{n_{\text{test}}}$ that was not observed during training.

We focus on generalizing the vision-language pre-trained model CLIP Radford *et al.* [2021] to unseen domains. During training, we fine-tune only the visual encoder f_I , while the CLIP text encoder remains frozen with class name text embeddings $\{T_c\}_{c=1}^C$ pre-encoded using prompt templates (e.g., “a photo of a {class name}”). This allows us to predict the class probabilities of the image x :

$$\mathcal{P}(y|x) = \frac{\exp(\langle f_I(x), T_y \rangle / \tau)}{\sum_{c=1}^C \exp(\langle f_I(x), T_c \rangle / \tau)} \quad (1)$$

where $\langle \cdot, \cdot \rangle$ represents the cosine similarity for normalized embeddings and τ is a temperature scaler. $f_I(x) \in \mathbb{R}^d$ is the image embedding for sample x .

3.2 Style-homogenized Alignment

Existing fine-tuning strategies for CLIP typically rely on direct alignment between image and text embeddings. However, such alignment may be mismatched due to extra domain-specific information encoded in the visual embeddings but not in the text embeddings, which can degrade the model’s ability to generalize to unseen domains. Accordingly, SHED focuses on aligning style-homogenized embeddings between image and text during fine-tuning:

$$\mathcal{L}_c = -\log \frac{\exp(\langle \hat{f}_I(x), \hat{T}_y \rangle / \tau)}{\sum_{c=1}^C \exp(\langle \hat{f}_I(x), \hat{T}_c \rangle / \tau)} \quad (2)$$

where $\hat{f}_I(x) \in \mathbb{R}^d$ and $\hat{T} \in \mathbb{R}^d$ represent the style-homogenized embeddings for images and texts.

Specifically, $\hat{f}_I(x)$ is computed by removing the domain centroid from the original image embedding:

$$\hat{f}_I(x) = \frac{f_I(x) - \mu_s}{\|f_I(x) - \mu_s\|}, \quad \mu_s = \frac{1}{n_s} \sum_{x \in \mathcal{D}^s} f_I(x) \quad (3)$$

where μ_s represents the centroid for domain s . It is obvious that the domain centroid captures the most concentrated or representative information of the domain Chen *et al.* [2023]; Liang *et al.* [2024]. When the domain centroid is removed from sample embeddings, the remaining style-homogenized embeddings are expected to preserve mainly class-specific information. It is worth noting that μ_s is computed prior to training via some passes over the training dataset, and it remains unchanged throughout the subsequent training. We argue that, since the initial model embeddings retain the semantic information of the original CLIP, fixing μ_s helps preserve CLIP’s strong generalization capability during later training.

Similarly, we apply templates $\{T_s\}_{s=1}^S$ (e.g., “a {domain name} photo of {class name}”, where domain styles are known during training such as “drawing” and “cartoon”) to each class and perform aggregation:

$$T_c = \frac{1}{S} \sum_{s=1}^S f_T(T_s(c)), \quad (4)$$

where f_T is the frozen text encoder from CLIP model. Then we can obtain the domain-invariant text embeddings:

$$\hat{T}_c = \frac{T_c - \mu^{\text{text}}}{\|T_c - \mu^{\text{text}}\|}, \quad \mu^{\text{text}} = \frac{1}{C} \sum_{c=1}^C T_c. \quad (5)$$

As shown in Figure 2a, $\hat{f}_I(x) \in \mathbb{R}^d$ and \hat{T}_c exhibit high similarity for their corresponding classes, indicating that style-homogenized embeddings are highly discriminative. Intuitively, subtracting centroids facilitates every domain to share a common structure, making cross-modal directions comparable. By aligning the model via Equation (2) during training, the discriminative power of style-homogenized embeddings can be further improved as illustrated by subtle deeper color in Figure 2c compared to Figure 2b. In our opinion, the minor differences between the two figures indicates that SHED largely preserves the powerful semantic representations of the original CLIP model, which facilitates generalization across broader domains.

Additionally, to ensure training stability and further retain the inherent generalization strength of CLIP, SHED regularizes the model by encouraging its embeddings to approximate the original CLIP embeddings:

$$\mathcal{L}_{\text{reg}} = \sum_{i=1}^d \|f_I(x) - f_I^{\text{CLIP}}(x)\| + \|\hat{f}_I(x) - \hat{f}_I^{\text{CLIP}}(x)\|, \quad (6)$$

where the superscript “CLIP” indicates that the embedding is produced by the original CLIP model, and d is explicitly defined as the dimension of the embedding. \mathcal{L}_{reg} employs $L1$ loss to simultaneously constrain both visual embeddings and style-homogenized embeddings. Its effect will be demonstrated in the ablation study. In summary, the total training objective is $\mathcal{L} = \mathcal{L}_c + \mathcal{L}_{\text{reg}}$.

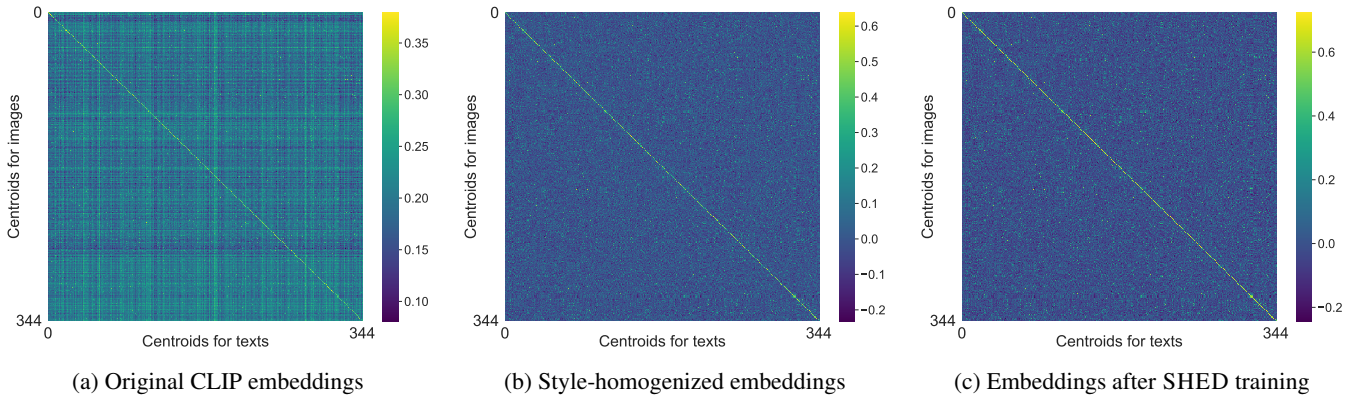


Figure 2: The heatmaps of cross-modal centroids similarities for “Clipart” domain in DomainNet Peng *et al.* [2019]. For clarity, the “image centroid” for each class is defined as the mean embedding within that class, and the “text centroid” for each class is defined as the mean embedding derived from multiple domain-styled prompt templates for that class.

Method	Venue	PACS	VLCS	OfficeHome	TerraInc	DomainNet	Avg
CLIP Zero-Shot	ICML’21	96.2	81.7	82.0	33.4	57.5	70.2
Style-Homogenized Zero-Shot	-	96.5	79.7	84.6	34.2	60.0	71.0
ERM	-	96.1±0.5	83.0±0.2	83.3±0.3	60.9±0.2	59.9±0.1	76.7±0.2
CoOp [Zhou <i>et al.</i> , 2022c]	IJCV’22	96.0 (-0.1)	81.1 (-1.9)	83.5 (+0.2)	47.0 (-13.9)	59.8 (-0.1)	73.5 (-3.2)
CoCoOp [Zhou <i>et al.</i> , 2022b]	CVPR’22	95.7 (-0.4)	83.1 (+0.1)	84.3 (+1.0)	50.4 (-10.5)	60.0 (+0.1)	74.7 (-2.0)
MIRO [Cha <i>et al.</i> , 2022]	ECCV’22	95.6 (-0.5)	82.2 (-0.8)	82.5 (-0.8)	54.3 (-6.6)	54.0 (-5.9)	73.7 (-3.0)
CLIPood [Shu <i>et al.</i> , 2023]	ICML’23	97.3±0.1 (+1.2)	85.0±0.4 (+2.0)	87.0±0.2 (+3.7)	60.4±0.7 (-0.5)	63.5±0.1 (+3.6)	78.6±0.2 (+1.9)
VLV2-SD [Addepalli <i>et al.</i> , 2024]	CVPR’24	96.7 (+0.6)	83.3 (+0.3)	87.4 (+4.1)	58.5 (-2.4)	62.8 (+2.9)	77.7 (+1.0)
CLIPCEIL [Yu <i>et al.</i> , 2024]	NeurIPS’24	97.2±0.1 (+1.1)	85.2±0.5 (+2.2)	87.7±0.3 (+4.4)	62.0±0.5 (+1.1)	63.6±0.2 (+3.7)	79.1±0.2 (+2.4)
Diverse Text Prompts [Wen <i>et al.</i> , 2025]	CVPR’25	97.0 (+0.9)	84.8 (+1.8)	87.7 (+4.4)	63.3 (+2.4)	63.1 (+3.2)	79.2 (+2.5)
SHED (ours)	-	97.6±0.1 (+1.5)	85.4±0.2 (+2.4)	87.7±0.1 (+4.4)	62.5±0.3 (+1.6)	63.9±0.1 (+4.0)	79.4±0.2 (+2.7)

Table 1: Comparison of classification accuracy on domain generalization benchmarks. Parentheses indicate the performance gap from the standard fine-tuning of CLIP (ERM), where values highlighted in green and gray indicate performance is better or worse than ERM. The best results are in bold.

3.3 Domain-Agnostic Centroid Aggregation

Although style-homogenized alignment enhances model’s ability to distinguish between classes, it is impractical to directly rely on style-homogenized embeddings during inference, as the domain of each test sample cannot be assumed. To solve this challenge, we propose to construct new textual domain centroids of multiple additional domain styles:

$$\mu_t = \frac{1}{C} \sum_{c=1}^C f_T(T_t(c)), \quad (7)$$

where $\{T_t\}_{t=1}^{N_T}$ is the templates for additional N_T domain styles and μ_t represents the centroid for template T_t . Additional domain styles are provided in the supplementary material. Considering the existing gap Liang *et al.* [2022] between visual and textual modalities in CLIP, we adopt two distinct approaches to project the corresponding textual centroids into the visual embedding space.

- **Centroids Projection Method (CPM).** CPM computes the relative difference between the additional text centroids and the S source domain centroids, and transfers this difference to the visual domain centroids μ_s :

$$\mu_t^{\text{CPM}} = \frac{1}{S} \sum_{s=1}^S \mu_s + (\mu_t - \mu_s^{\text{text}}), \quad (8)$$

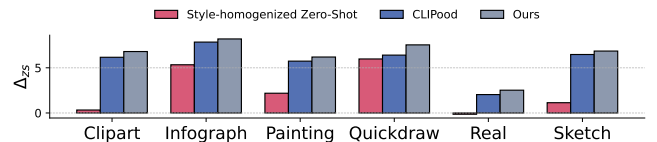


Figure 3: Performance change of different methods relative to the zero-shot CLIP baseline under various domains on DomainNet.

where $\mu_s^{\text{text}} = \frac{1}{C} \sum_{c=1}^C f_T(T_s(c))$ represents the centroids for source domain s .

- **Sample Weighting Method (SWM).** SWM utilizes similarity between new text centroids and visual sample embeddings as weights, and derives visual centroids of additional styles by aggregating weighted visual embeddings:

$$\mu_t^{\text{SWM}} = \left(\text{softmax} \left(\frac{\mu_t \cdot V^{\text{CLIP}}}{\tau_{\text{SWM}}} \right) \right) \cdot V^{\text{CLIP}}, \quad (9)$$

where temperature parameter τ_{SWM} is set to a default value of $\frac{1}{100}$. Notably, V^{CLIP} is the visual embeddings sampled before training process begins.

We posit that these two complementary projection methods can bridge the modality gap robustly. CPM operates on

Ablations	Clipart	Infograph	Painting	Quickdraw	Real	Sketch	Avg
SHED	78.2	54.8	72.9	21.3	85.8	70.4	63.9
w/o Style-homogenized alignment	76.9 (-1.3)	53.8 (-1.0)	71.4 (-1.5)	21.1 (-0.2)	85.6 (-0.2)	69.0 (-1.4)	63.0 (-0.9)
w/o Regularization	78.6 (+0.4)	53.9 (-0.9)	72.4 (-0.5)	20.3 (-1.0)	85.6 (-0.2)	69.6 (-0.8)	63.4 (-0.5)
w/o Combined predictions	78.2 (-0.0)	54.5 (-0.3)	72.5 (-0.4)	21.1 (-0.2)	84.6 (-1.2)	70.1 (-0.3)	63.5 (-0.4)
w/o Additional centroids	78.2 (-0.0)	54.5 (-0.3)	72.5 (-0.4)	20.6 (-0.7)	85.7 (-0.1)	70.1 (-0.3)	63.6 (-0.3)
w/o CPM	78.3 (+0.1)	54.6 (-0.2)	72.8 (-0.1)	20.6 (-0.7)	85.7 (-0.1)	70.3 (-0.1)	63.7 (-0.2)
w/o SWM	78.1 (-0.1)	54.2 (-0.6)	72.7 (-0.2)	21.3 (-0.0)	85.7 (-0.1)	70.3 (-0.1)	63.7 (-0.2)

Table 2: Ablation studies. We investigate the impact of the core components of the SHED on DomainNet. “w/o Style-homogenized alignment” represents that Equation (2) is replaced by direct alignment of image and text features. The regularization denotes the loss in Equation (6). Parentheses indicate the performance gap from SHED, where values highlighted in green and gray indicate performance is better or worse than SHED, respectively.

Algorithm 1 SHED Training

Require: Source domains \mathcal{D}^s for $s = 1$ to S , number of iterations E

Require: Pre-trained CLIP encoders f_I, f_T

- 1: Compute centroid $\mu_s \leftarrow \text{mean}(f_I^{\text{CLIP}}(x))$ for each domain s
- 2: $T_c \leftarrow \frac{1}{S} \sum_{s=1}^S f_T(\text{“a [domain] photo of a \{c\}”})$
- 3: Compute global text centroid $\mu^{\text{text}} \leftarrow \text{mean}(T_c)$
- 4: $\hat{T}_c \leftarrow \text{Normalize}(T_c - \mu^{\text{text}})$
- 5: **for** $e = 1$ **to** E **do**
- 6: Sample batch (x, y, s)
- 7: Extract $f_I(x)$
- 8: $\hat{f}_I(x) \leftarrow \text{normalize}(f_I(x) - \mu_s)$
- 9: Compute \mathcal{L}_c through Equation (2)
- 10: Compute \mathcal{L}_{reg} through Equation (6)
- 11: Update f_I using $\nabla(\mathcal{L}_c + \mathcal{L}_{reg})$
- 12: **end for**

a global level, assuming a consistent structural relationship by transferring a relative “style vector” from the text space to the visual space. In contrast, SWM takes a more localized, data-driven method, constructing a visual style centroid by attending to source images that are semantically closest to the target style description. By combining both, SHED synthesizes a richer and more accurate set of potential visual domain centroids for inference.

After obtaining a sufficient number of visual domain centroids, the next step is to assign domain centroids for each test sample $x_j \in \mathcal{D}^{\text{test}}$ in inference. SHED first combines all visual centroids, i.e., $\mu^V = \text{concat}(\{\mu_s\}_{s=1}^S, \{\mu_t^{\text{CPM}}\}_{t=1}^{N_T}, \{\mu_t^{\text{SWM}}\}_{t=1}^{N_T})$, and then computes the soft assignment of $f_I^{\text{CLIP}}(x_j)$ to all centroids:

$$\pi_j = \text{softmax}\left(\frac{f_I^{\text{CLIP}}(x_j) \cdot \mu^V}{\tau_c}\right), \quad (10)$$

where τ_c is the temperature for centroids assignment. It is evident that π_j places greater emphasis on centroids more aligned with the style of x_j and can serve as a membership weighting for each domain centroid during inference.

Subsequently, sample x_j utilizes each element in $\mu^V = \{\mu_v^V\}_{v=1}^{2N_T+S}$ as domain centroid to compute the corresponding prediction $\mathcal{P}_v(y|x_j, \mu_v^V)$ following the probability inside

Algorithm 2 SHED Inference

Require: Test sample x_j

Require: style-homogenized text embeddings $\{\hat{T}_c\}$

- 1: **Construct visual centroids:**
- 2: **for** each domain style t **do**
- 3: $\mu_t^{\text{CPM}} \leftarrow \text{project via CPM}$
- 4: $\mu_t^{\text{SWM}} \leftarrow \text{project via SWM}$
- 5: **end for**
- 6: $\mu^V \leftarrow \{\mu_s\} \cup \{\mu_t^{\text{CPM}}\} \cup \{\mu_t^{\text{SWM}}\}$
- 7: **Compute predictions:**
- 8: $\pi_j \leftarrow \text{softmax}(f_I^{\text{CLIP}}(x_j) \cdot \mu^V)$
- 9: **for** each centroid $\mu_v \in \mu^V$ **do**
- 10: $\hat{f}_I \leftarrow \text{normalize}(f_I(x_j) - \mu_v)$
- 11: $\mathcal{P}_v(y|x_j) \leftarrow \text{softmax}(\langle \hat{f}_I, \hat{T}_y \rangle)$
- 12: **end for**
- 13: $\mathcal{P}^\mu \leftarrow \sum_v \pi_j(v) \cdot \mathcal{P}_v(y|x_j)$
- 14: **Final prediction:** $\mathcal{P} \leftarrow \lambda \cdot \mathcal{P}^{\text{CLIP}} + (1 - \lambda) \cdot \mathcal{P}^\mu$
- 15: **return** $\arg \max_y \mathcal{P}(y|x_j)$

the negative logarithm in Equation (2) and integrate the predictions using soft assignment from π_j :

$$\mathcal{P}^\mu(y|x_j) = \sum_{v=1}^{2N_T+S} \pi_j(v) \cdot \mathcal{P}_v(y|x_j, \mu_v^V). \quad (11)$$

Meanwhile, considering the strong zero-shot capability of CLIP, we combine the inference probabilities $\mathcal{P}(y|x_j)$ with its zero-shot prediction $\mathcal{P}^{\text{CLIP}}(y|x_j)$:

$$\mathcal{P}(y|x_j) = \mathcal{P}^{\text{CLIP}}(y|x_j) \cdot \lambda(x_j) + \mathcal{P}^\mu(y|x_j) \cdot (1.0 - \lambda(x_j)), \quad (12)$$

where $\lambda(x_j) = \max_{1 \leq c \leq C} \mathcal{P}^{\text{CLIP}}(c|x)$ is the confidence of the zero-shot CLIP prediction for x_j . When zero-shot CLIP is confident in its prediction, the final decision is primarily guided by CLIP; otherwise, it is dominated by $\mathcal{P}^\mu(y|x_j)$. In summary, the overall training and inference procedures of SHED are presented in Algorithm 1 and Algorithm 2 respectively.

4 Experiments

In this section, we demonstrate that the proposed SHED method achieves consistent improvements on domain generalization benchmarks compared to previous methods. We

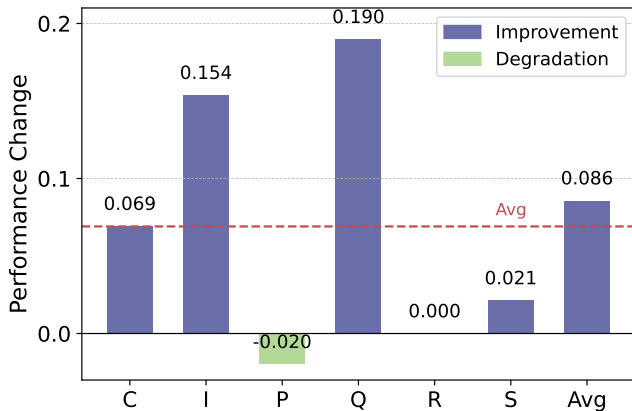


Figure 4: Performance change by incorporating additional centroids derived from real target domain style words into SHED. “C”, “I”, “P”, “Q”, “R”, and “S” represent the first letters of the six target domains in the DomainNet.

also provide an in-depth analysis of the method and conduct ablation studies to investigate the contribution of each component to overall performance.

4.1 Datasets and Evaluation Metrics

To assess the effectiveness of our approach, we perform evaluations on five standard domain generalization benchmarks, including PACS Li *et al.* [2017], VLCS Torralba and Efros [2011], OfficeHome Venkateswara *et al.* [2017], TerraIncognita Beery *et al.* [2018], and DomainNet Peng *et al.* [2019]. PACS consists of 9,991 images from 7 object categories across 4 distinct domains (Photo, Art painting, Cartoon, and Sketch). VLCS comprises 10,729 images spanning 5 categories from 4 domains, drawn from multiple classical computer vision datasets. OfficeHome contains 15,579 images from 65 object categories in 4 domains (Art, Clipart, Product, and Real-World). TerraIncognita includes 24,788 wildlife images from 10 categories across 4 geographic domains, highlighting domain shifts due to environmental differences. DomainNet, the largest and most challenging benchmark, contains approximately 600,000 images from 345 categories in 6 diverse domains (Clipart, Infograph, Painting, Quickdraw, Real, and Sketch), introducing significant challenges in both domain and category shifts. The performance is measured by Top-1 classification accuracy (%) on novel domain dataset $\mathcal{D}^{\text{test}}$. Results are reported as the mean and standard deviation across three random seeds.

4.2 Implementation Details

Following previous method Shu *et al.* [2023], we use pre-trained CLIP ViT-B/16 Dosovitskiy *et al.* [2020]; Radford *et al.* [2021] as backbone. The image encoder is full fine-tuned and the text encoder is frozen during training. In our experiments, the parameter τ in Equation (2) was set to $\frac{1}{20}$ for the DomainNet dataset, and to $\frac{1}{5}$ for the other datasets. Unless otherwise specified, both temperature parameters τ_{SWM} and τ_{C} were fixed at $\frac{1}{100}$ across all datasets. We employ the AdamW optimizer Loshchilov and Hutter [2017] along with

cosine learning rate schedule for all datasets. Additional experimental details can be found in supplementary material.

4.3 Main Results

We conduct extensive comparisons with state-of-the-art methods on five widely-used benchmark datasets to evaluate the effectiveness of SHED, and the results are shown in Table 1. We provide the results of CLIP zero-shot, style-homogenized zero-shot, and standard fine-tuning for CLIP pre-trained model (ERM). Across the majority of datasets, style-homogenized zero-shot demonstrates superior performance compared to CLIP zero-shot, yielding an average gain of around 0.84%. We also compare our method with recent domain generalization approaches based on the pretrained CLIP model, including CLIPood [Shu *et al.*, 2023], VLV2-SD [Addepalli *et al.*, 2024], and CLIPCEIL [Yu *et al.*, 2024]. Overall, we argue that our results are significant, especially given the high difficulty of DG tasks. SHED consistently outperforms all competing methods across all five benchmarks. This consistency is a critical differentiator; in contrast, competing methods like CLIPood and CLIPCEIL failed to show consistent or significant gains across all tested scenarios. Remarkably, SHED achieves an average performance gain of 2.7% over ERM, with considerable gains of 4.4% on OfficeHome and 4.0% on DomainNet. It is particularly worth emphasizing that SHED surpasses the state-of-the-art CLIPCEIL by 0.5 and 0.3 on TerraIncognita and DomainNet, respectively. These datasets are known for their difficulty due to wild imagery and large category diversity, indicating the robustness of SHED in complex settings. Detailed results for each domain within datasets, along with further analysis, are provided in supplementary material.

4.4 Analysis of SHED

Ablation Analysis. To comprehensively understand the contribution of each component within our proposed SHED, we present a detailed ablation study in Table 2. Notably, replacing our style-homogenized alignment with image-text alignment loss during training leads to a significant degradation in performance across all domains. The most pronounced drop is observed in the “Painting” domain, which experiences a 1.5% performance decrease. This evidence indicates that style-homogenized alignment is instrumental in bolstering the model’s robustness and its capacity for generalization when encountering out-of-distribution domains. The removal of alignment regularization and prediction combination from the original CLIP model resulted in a performance drop of 0.4% to 0.5%, indicating that semantic support from CLIP facilitates the model’s generalization across various complex domains. When removing additional centroids, the model suffered a performance degradation, with the “Quickdraw” domain experiencing the most pronounced drop of 0.7%. Given the inherent difficulty of “Quickdraw” as a target domain Kempf *et al.* [2025], this underscores the substantial contribution of additional centroids to the accurate prediction of stylistically anomalous samples. Furthermore, the removal of either CPM or SWM resulted in a measurable decrease in the model’s generalization performance,

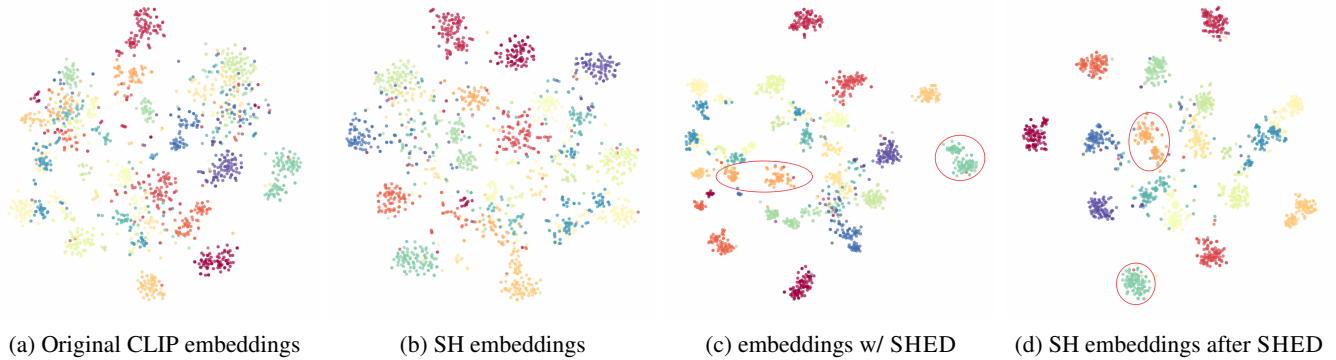


Figure 5: The t-SNE visualization of embeddings on DomainNet. SH is an abbreviation for style-homogenized.

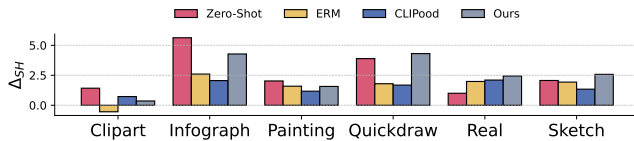


Figure 6: Performance change Δ_{SH} before and after applying style-homogenized inference on DomainNet.

which emphasizes the necessity of generating diverse additional centroids to generalize to more style domains.

Analysis on Performance Change. In Figure 3, we present the performance changes of different methods relative to CLIP zero-shot on DomainNet. We observe that zero-shot performance using style-homogenized embeddings significantly outperforms original zero-shot, further demonstrating the effectiveness of style-homogenized embeddings in addressing domain shift. Moreover, SHED achieves the best performance, and the performance advantage is more pronounced on domains such as “Infograph” and “Quickdraw”, which exhibit greater divergence from natural image styles and existing domain generalization methods fail to achieve competitive performance under these circumstances.

Analysis on Additional Centroids. During the construction of additional centroids in SHED, a large number of domain-specific style words are utilized, covering common domain styles, which may potentially include the real style of the target domain. This highlights the importance of examining how real target domain word influences the model’s performance. Figure 4 shows the performance difference of SHED compared to its variant that constructs centroids without using real target domain style word. While the use of true domain-style terms leads to consistent improvements across most target domains, the overall performance gain is marginal, remaining under 0.1%. This suggests that SHED does not rely on true domain-specific style words and can instead enhance model robustness through the use of a large and diverse set of domain words. Additionally, we observe that domains “Infograph” and “Quickdraw” are slightly more sensitive to the inclusion of real domain-specific words, which is primarily attributed to the significant disparity between these two domains and common domains. This offers flexibility to our

method: if the approximate domain style is known especially for the rare styles, incorporating corresponding domain words into centroids construction can further improve generalization to the target domain.

Analysis on Embedding Visualizations. We visualize image and style-homogenized embeddings using t-SNE Van der Maaten and Hinton [2008] in Figure 5. Comparing Figure 5a and Figure 5b before training, we observe that style-homogenized embeddings exhibit better class separability than original embeddings, suggesting that style information in original embeddings may negatively impact classification performance. After training with SHED a comparison between Figure 5c and Figure 5d (highlighted in red) reveals that style-homogenized embeddings form more compact class clusters than image embeddings, showing its robustness under domains with unusual or unseen styles.

Analysis on Domain-Agnostic Centroid Aggregation. To analyze the impact of domain-agnostic centroid aggregation inference on different methods, we present in Figure 6 the performance differences compared to direct prediction using image-text embeddings. The results indicate that domain-agnostic centroid aggregation inference leads to more pronounced improvements for zero-shot and SHED on the majority of target domains, highlighting the effectiveness of SHED in preserving CLIP’s inherent representational structure, which is crucial for synthesizing style-homogenized embeddings. ERM and CLIPood exhibit relatively limited performance gains, which we attribute to the asymmetric image-text alignment that partially disrupts the representational structure of the original CLIP model, thereby leading to significant deviations in the construction of style-homogenized embeddings.

5 Conclusion

This paper introduces SHED, a novel CLIP-based approach for domain generalization. SHED addresses the critical limitation of asymmetric information between images (containing class+style) and text (containing only class) by aligning style-homogenized embeddings instead of raw representations. It removes domain-specific style centroids from both modalities during training. For inference without target domain labels, SHED projects diverse text domain centroids into the visual

space and aggregates predictions via soft assignment. Extensive experiments on five benchmarks demonstrate that SHED achieves state-of-the-art performance, significantly outperforming prior methods. We argue that SHED introduces a novel perspective that sheds light on how pre-trained models can be more effectively exploited for domain generalization tasks.

References

- Sravanti Addepalli, Ashish Ramayee Asokan, Lakshay Sharma, and R Venkatesh Babu. Leveraging vision-language models for improving domain generalization in image classification. In *Proceedings of the IEEE/CVF Conference on Computer Vision and Pattern Recognition*, pages 23922–23932, 2024.
- Sara Beery, Grant Van Horn, and Pietro Perona. Recognition in terra incognita. In *Proceedings of the European Conference on Computer Vision (ECCV)*, pages 456–473, 2018.
- Manh-Ha Bui, Toan Tran, Anh Tran, and Dinh Phung. Exploiting domain-specific features to enhance domain generalization. *Advances in Neural Information Processing Systems*, 34:21189–21201, 2021.
- Junbum Cha, Kyungjae Lee, Sungrae Park, and Sanghyuk Chun. Domain generalization by mutual-information regularization with pre-trained models. In *European Conference on Computer Vision*, pages 440–457. Springer, 2022.
- Shoufa Chen, Chongjian Ge, Zhan Tong, Jiangliu Wang, Yibing Song, Jue Wang, and Ping Luo. Adaptformer: Adapting vision transformers for scalable visual recognition. *Advances in Neural Information Processing Systems*, 35:16664–16678, 2022.
- Tianle Chen, Mahsa Baktashmotlagh, Zijian Wang, and Mathieu Salzmann. Center-aware adversarial augmentation for single domain generalization. In *Proceedings of the IEEE/CVF Winter Conference on Applications of Computer Vision*, pages 4157–4165, 2023.
- Bowen Dong, Pan Zhou, Shuicheng Yan, and Wangmeng Zuo. Lpt: Long-tailed prompt tuning for image classification. *arXiv preprint arXiv:2210.01033*, 2022.
- Alexey Dosovitskiy, Lucas Beyer, Alexander Kolesnikov, Dirk Weissenborn, Xiaohua Zhai, Thomas Unterthiner, Mostafa Dehghani, Matthias Minderer, Georg Heigold, Sylvain Gelly, et al. An image is worth 16x16 words: Transformers for image recognition at scale. *arXiv preprint arXiv:2010.11929*, 2020.
- Ruoyu Feng, Tao Yu, Xin Jin, Xiaoyuan Yu, Lei Xiao, and Zhibo Chen. Rethinking domain adaptation and generalization in the era of clip. In *2024 IEEE International Conference on Image Processing (ICIP)*, pages 2585–2591. IEEE, 2024.
- Kai Gan and Tong Wei. Erasing the bias: fine-tuning foundation models for semi-supervised learning. In *Proceedings of the 41st International Conference on Machine Learning*, pages 14453–14470, 2024.
- Kai Gan, Bo Ye, Min-Ling Zhang, and Tong Wei. Semi-supervised clip adaptation by enforcing semantic and trapezoidal consistency. In *The Thirteenth International Conference on Learning Representations*, 2025.
- Neil Houlsby, Andrei Giurgiu, Stanislaw Jastrzebski, Bruna Morrone, Quentin De Laroussilhe, Andrea Gesmundo, Mona Attariyan, and Sylvain Gelly. Parameter-efficient transfer learning for nlp. In *International Conference on Machine Learning*, pages 2790–2799. PMLR, 2019.
- Chao Jia, Yinfei Yang, Ye Xia, Yi-Ting Chen, Zarana Parekh, Hieu Pham, Quoc Le, Yun-Hsuan Sung, Zhen Li, and Tom Duerig. Scaling up visual and vision-language representation learning with noisy text supervision. In *International Conference on Machine Learning*, pages 4904–4916. PMLR, 2021.
- Menglin Jia, Luming Tang, Bor-Chun Chen, Claire Cardie, Serge Belongie, Bharath Hariharan, and Ser-Nam Lim. Visual prompt tuning. In *European Conference on Computer Vision*, pages 709–727. Springer, 2022.
- Elias Kempf, Simon Schrodi, Max Argus, and Thomas Brox. When and how does clip enable domain and compositional generalization? *arXiv preprint arXiv:2502.09507*, 2025.
- Zhengfeng Lai, Noranart Vespapunt, Ning Zhou, Jun Wu, Cong Phuoc Huynh, Xuelu Li, Kah Kuen Fu, and Chen-Nee Chuah. Padclip: Pseudo-labeling with adaptive debiasing in clip for unsupervised domain adaptation. In *Proceedings of the IEEE/CVF International Conference on Computer Vision*, pages 16155–16165, 2023.
- Da Li, Yongxin Yang, Yi-Zhe Song, and Timothy M Hospedales. Deeper, broader and artier domain generalization. In *Proceedings of the IEEE International Conference on Computer Vision*, pages 5542–5550, 2017.
- Haoliang Li, Sinno Jialin Pan, Shiqi Wang, and Alex C Kot. Domain generalization with adversarial feature learning. In *Proceedings of the IEEE Conference on Computer Vision and Pattern Recognition*, pages 5400–5409, 2018.
- Ya Li, Xinmei Tian, Mingming Gong, Yajing Liu, Tongliang Liu, Kun Zhang, and Dacheng Tao. Deep domain generalization via conditional invariant adversarial networks. In *Proceedings of the European Conference on Computer Vision (ECCV)*, pages 624–639, 2018.
- Junnan Li, Ramprasaath Selvaraju, Akhilesh Gotmare, Shafiq Joty, Caiming Xiong, and Steven Chu Hong Hoi. Align before fuse: Vision and language representation learning with momentum distillation. *Advances in Neural Information Processing Systems*, 34:9694–9705, 2021.
- Junnan Li, Dongxu Li, Caiming Xiong, and Steven Hoi. Blip: Bootstrapping language-image pre-training for unified vision-language understanding and generation. In *International Conference on Machine Learning*, pages 12888–12900. PMLR, 2022.
- Junnan Li, Dongxu Li, Silvio Savarese, and Steven Hoi. Blip-2: Bootstrapping language-image pre-training with frozen image encoders and large language models. In *International Conference on Machine Learning*, pages 19730–19742. PMLR, 2023.

- Victor Weixin Liang, Yuhui Zhang, Yongchan Kwon, Serena Yeung, and James Y Zou. Mind the gap: Understanding the modality gap in multi-modal contrastive representation learning. *Advances in Neural Information Processing Systems*, 35:17612–17625, 2022.
- Jiachen Liang, RuiBing Hou, Minyang Hu, Hong Chang, Shiguang Shan, and Xilin Chen. Umfc: Unsupervised multi-domain feature calibration for vision-language models. In *The Thirty-eighth Annual Conference on Neural Information Processing Systems*, 2024.
- Ilya Loshchilov and Frank Hutter. Decoupled weight decay regularization. *arXiv preprint arXiv:1711.05101*, 2017.
- Mao-Lin Luo, Zi-Hao Zhou, Tong Wei, and Min-Ling Zhang. LADA: Scalable label-specific CLIP adapter for continual learning. In *Forty-second International Conference on Machine Learning*, 2025.
- Hyeonseob Nam, HyunJae Lee, Jongchan Park, Wonjun Yoon, and Donggeun Yoo. Reducing domain gap by reducing style bias. In *Proceedings of the IEEE/CVF Conference on Computer Vision and Pattern Recognition*, pages 8690–8699, 2021.
- David Osowiechi, Mehrdad Noori, Gustavo Adolfo Vargas Hakim, Moslem Yazdanpanah, Ali Bahri, Milad Cheraghlikhani, Sahar Dastani, Farzad Beizae, Ismail Ben Ayed, and Christian Desrosiers. Watt: Weight average test-time adaptation of clip. *arXiv preprint arXiv:2406.13875*, 2024.
- Xingchao Peng, Qinxun Bai, Xide Xia, Zijun Huang, Kate Saenko, and Bo Wang. Moment matching for multi-source domain adaptation. In *Proceedings of the IEEE/CVF International Conference on Computer Vision*, pages 1406–1415, 2019.
- Hieu Pham, Zihang Dai, Golnaz Ghiasi, Kenji Kawaguchi, Hanxiao Liu, Adams Wei Yu, Jiahui Yu, Yi-Ting Chen, Minh-Thang Luong, Yonghui Wu, et al. Combined scaling for zero-shot transfer learning. *Neurocomputing*, 555:126658, 2023.
- Alec Radford, Jong Wook Kim, Chris Hallacy, Aditya Ramesh, Gabriel Goh, Sandhini Agarwal, Girish Sastry, Amanda Askell, Pamela Mishkin, Jack Clark, et al. Learning transferable visual models from natural language supervision. In *International Conference on Machine Learning*, pages 8748–8763. PMLR, 2021.
- Mattia Segu, Alessio Tonioni, and Federico Tombari. Batch normalization embeddings for deep domain generalization. *Pattern Recognition*, 135:109115, 2023.
- Jiang-Xin Shi, Tong Wei, Zhi Zhou, Jie-Jing Shao, Xin-Yan Han, and Yu-Feng Li. Long-tail learning with foundation model: heavy fine-tuning hurts. In *International Conference on Machine Learning*, pages 45014–45039. PMLR, 2024.
- Yang Shu, Xingzhuo Guo, Jialong Wu, Ximei Wang, Jianmin Wang, and Mingsheng Long. Clipood: Generalizing clip to out-of-distributions. In *International Conference on Machine Learning*, pages 31716–31731. PMLR, 2023.
- Antonio Torralba and Alexei A Efros. Unbiased look at dataset bias. In *CVPR 2011*, pages 1521–1528. IEEE, 2011.
- Laurens Van der Maaten and Geoffrey Hinton. Visualizing data using t-sne. *Journal of Machine Learning Research*, 9(11), 2008.
- Hemanth Venkateswara, Jose Eusebio, Shayok Chakraborty, and Sethuraman Panchanathan. Deep hashing network for unsupervised domain adaptation. In *Proceedings of the IEEE Conference on Computer Vision and Pattern Recognition*, pages 5018–5027, 2017.
- Tong Wei, Hao-Tian Li, Chun-Shu Li, Jiang-Xin Shi, Yu-Feng Li, and Min-Ling Zhang. Vision-language models are strong noisy label detectors. *Advances in Neural Information Processing Systems*, 37:58154–58173, 2024.
- Tong Wei, Bolin Wang, Jiang-Xin Shi, Yu-Feng Li, and Min-Ling Zhang. X-mahalanobis: Transformer feature mixing for reliable ood detection. *Advances in Neural Information Processing Systems*, 38:141958–141986, 2026.
- Changsong Wen, Zelin Peng, Yu Huang, Xiaokang Yang, and Wei Shen. Domain generalization in clip via learning with diverse text prompts. In *Proceedings of the IEEE/CVF Conference on Computer Vision and Pattern Recognition*, pages 9559–9569, 2025.
- Size Wu, Wenwei Zhang, Lumin Xu, Sheng Jin, Xiangtai Li, Wentao Liu, and Chen Change Loy. Clipself: Vision transformer distills itself for open-vocabulary dense prediction. *arXiv preprint arXiv:2310.01403*, 2023.
- Xi Yu, Shinjae Yoo, and Yuewei Lin. Clipceil: Domain generalization through clip via channel refinement and image-text alignment. *Advances in Neural Information Processing Systems*, 37:4267–4294, 2024.
- Kaiyang Zhou, Ziwei Liu, Yu Qiao, Tao Xiang, and Chen Change Loy. Domain generalization: A survey. *IEEE Transactions on Pattern Analysis and Machine Intelligence*, 45(4):4396–4415, 2022.
- Kaiyang Zhou, Jingkang Yang, Chen Change Loy, and Ziwei Liu. Conditional prompt learning for vision-language models. In *Proceedings of the IEEE/CVF Conference on Computer Vision and Pattern Recognition*, pages 16816–16825, 2022.
- Kaiyang Zhou, Jingkang Yang, Chen Change Loy, and Ziwei Liu. Learning to prompt for vision-language models. *International Journal of Computer Vision*, 130(9):2337–2348, 2022.
- Zhi Zhou, Lan-Zhe Guo, Lin-Han Jia, Dingchu Zhang, and Yu-Feng Li. Ods: Test-time adaptation in the presence of open-world data shift. In *International Conference on Machine Learning*, pages 42574–42588. PMLR, 2023.

Supplementary Material

We provide supplementary material to facilitate a better understanding of the proposed SHED.

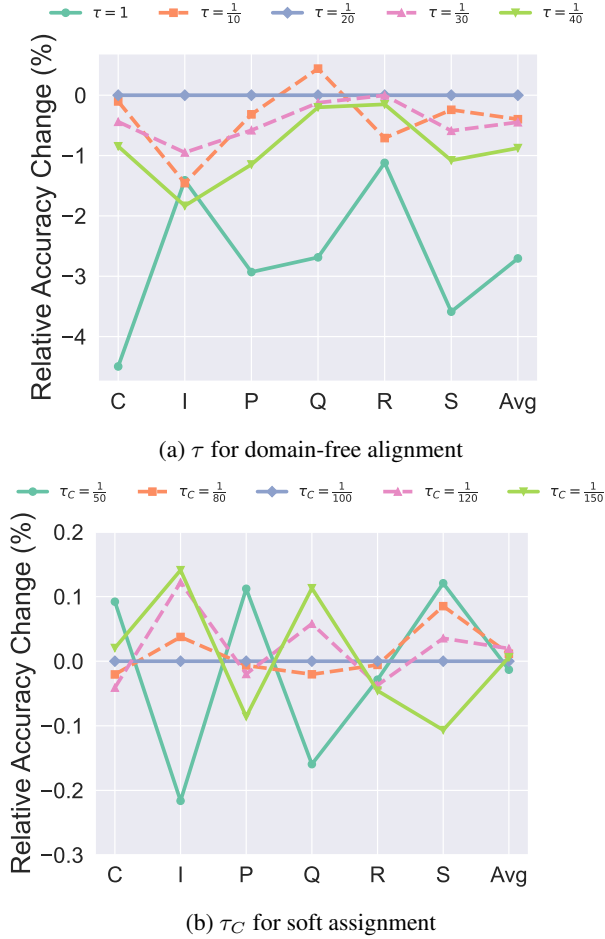


Figure 7: The sensitivity of τ and τ_C under various settings on DomainNet.

A More Implementation Details

In this section, we provide additional implementation details of SHED. To ensure a fair comparison, we follow the most experimental setup of CLIPood. Given the relatively larger data volume of DomainNet, we train SHED for 20 epochs, whereas only 10 epochs are used for the other datasets. We train for 500 iterations per epoch. We employ the AdamW optimizer along with a cosine learning rate schedule for all datasets. We set the learning rate to 1×10^{-5} for DomainNet and OfficeHome, and to 5×10^{-6} for the other datasets. Due to the sensitivity of the model to alignment strength, we choose $\tau = \frac{1}{20}$ for DomainNet and $\tau = \frac{1}{5}$ for the remaining datasets. We hypothesize that the large scale of DomainNet necessitates a stronger alignment strength to maintain the model structure for learning domain-free features. The temperature parameters τ_{SWM} is fixed at $\frac{1}{100}$ across all datasets. We set $\tau_C = \frac{1}{20}$ for VLCS and $\tau_C = \frac{1}{5}$ for TerraIncognita,

while using $\tau_C = \frac{1}{100}$ for all other datasets. For each result of SHED, we report the average result and the standard deviation of three runs with random seeds.

B Templates for Additional Centroids

We present in Table 3 the templates employed for constructing the additional centroids.

Template Prompt	
a drawing photo of a {}	a watercolor photo of a {}
a oil photo of a {}	a graffiti photo of a {}
a collage photo of a {}	a vector photo of a {}
a pixel photo of a {}	a minimalist photo of a {}
a abstract photo of a {}	a chart photo of a {}
a diagram photo of a {}	a blueprint photo of a {}
a surreal photo of a {}	a monochrome photo of a {}
a doodle photo of a {}	a clipart photo of a {}
a infograph photo of a {}	a painting photo of a {}
a quickdraw photo of a {}	a real photo of a {}
a sketch photo of a {}	a art photo of a {}
a product photo of a {}	a real world photo of a {}
a cartoon photo of a {}	a art painting photo of a {}
a white photo of a {}	a impressionist photo of a {}
a photorealistic photo of a {}	a vintage photo of a {}
a modern photo of a {}	a neon photo of a {}
a 3D photo of a {}	a pop art photo of a {}
a glitch photo of a {}	a isometric photo of a {}
a digital photo of a {}	an anime photo of a {}
a manga photo of a {}	a concept art photo of a {}
a futuristic photo of a {}	a cinematic photo of a {}
an abstract expressionism photo of a {}	an action painting photo of a {}
an art deco photo of a {}	an art nouveau photo of a {}
a baroque photo of a {}	a bauhaus photo of a {}
a cubism photo of a {}	an expressionism photo of a {}
a fauvism photo of a {}	an impressionism photo of a {}
a minimalism photo of a {}	a op art photo of a {}
a pointillism photo of a {}	a realism photo of a {}
a rococo photo of a {}	a surrealism photo of a {}

Table 3: Templates prompts for additional centroids.

C Sensitivity Analysis

Figure 7 presents the results of a sensitivity analysis on several parameters within SHED. τ serves as the temperature parameter for domain-free alignment, and we set $\tau = \frac{1}{20}$ on DomainNet. As shown in Figure 7a, the performance of the model is negatively affected when the temperature parameter τ is set either too low or too high. We conjecture that a

Method	Art	Cartoon	Photo	Sketch	Avg
CLIP Zero-Shot	97.3	99.1	99.9	88.3	96.2
CoOp	98.3	98.8	99.7	87.3	96.0
CoCoOp	97.6	98.6	99.7	87.0	95.7
MIRO	-	-	-	-	95.6
CLIPood	98.5	99.4	100.0	91.3	97.3
CLIPCEIL	-	-	-	-	97.2
SHED (ours)	98.9\pm0.1	99.6\pm0.0	100.0\pm0.0	91.9\pm0.1	97.6\pm0.1

Table 4: Comparison of classification accuracy on PACS. The best results are in **bold**.

Method	Caltech	LabelMe	Sun	Pascal	Avg
CLIP Zero-Shot	98.9	65.5	77.6	84.5	81.7
CoOp	97.9	65.5	76.6	84.3	81.1
CoCoOp	99.8	67.0	78.5	87.1	83.1
MIRO	-	-	-	-	82.2
CLIPood	100.0	67.7	80.2	92.1	84.8
CLIPCEIL	-	-	-	-	85.2
SHED (ours)	100.0\pm0.0	68.3\pm0.4	80.7\pm0.2	92.4\pm0.3	85.4\pm0.2

Table 5: Comparison of classification accuracy on VLCS. The best results are in **bold**.

large τ value reduces the sharpness of the similarity distribution, thereby weakening the alignment and impeding the learning of class-discriminative features. When τ is set too low, the alignment becomes overly aggressive, which may lead to overfitting to noisy or uncertain image samples. Overall, setting $\tau = \frac{1}{20}$ achieves a good balance in the strength of domain-free alignment. Additional, as we vary τ_C during the soft assignment process, the results in Figure 7b show no significant performance fluctuation, indicating that τ_c exhibits strong robustness.

D Full Results for Each Dataset

Tables 4 to 8 present the detailed results on the PACS, VLCS, OfficeHome, TerraIncognita, and DomainNet datasets. SHED achieves the best performance in most settings across each dataset. It is noteworthy that on datasets like PACS and VLCS, CoOp yields lower performance than CLIP zero-shot, indicating that such domain adaptation methods can significantly impair CLIP’s inherent generalization capability. However, SHED exhibits consistently superior performance, with an average improvement of 9.2% over CLIP zero-shot. We report the mean and standard deviation across three runs for SHED.

Method	Art	Clipart	Product	Real	Avg
CLIP Zero-Shot	82.7	68.0	88.3	90.7	82.4
CoOp	82.8	69.7	91.0	90.6	83.5
CoCoOp	83.9	70.0	91.4	91.9	84.3
MIRO	-	-	-	-	82.5
CLIPood	87.5	74.1	93.2	93.1	87.0
CLIPCEIL	-	-	-	-	87.7
SHED (ours)	88.3\pm0.1	75.0\pm0.1	93.9\pm0.1	93.5 \pm 0.1	87.7\pm0.1

Table 6: Comparison of classification accuracy on OfficeHome. The best results are in **bold**.

Method	L100	L38	L43	L46	Avg
CLIP Zero-Shot	51.2	23.4	29.9	29.1	33.4
CoOp	41.4	53.7	48.9	44.6	47.0
CoCoOp	50.7	56.0	51.9	44.0	50.4
MIRO	-	-	-	-	54.3
CLIPood	73.9	63.6	57.5	46.6	60.4
CLIPCEIL	-	-	-	-	62.0
SHED (ours)	75.9\pm0.5	66.4\pm0.8	59.4\pm0.3	48.4\pm0.6	62.5\pm0.3

Table 7: Comparison of classification accuracy on TerraIncognita. The best results are in **bold**.

E Additional Experimental Analysis

E.1 Inference Efficiency

To assess the practical applicability of SHED, we analyzed its computational cost during inference compared to the standard CLIP zero-shot method. The evaluation was performed on a single NVIDIA A100 GPU, measuring the average time to process one sample from the DomainNet dataset.

As shown in Table 9, SHED introduces a minimal computational overhead of only 8.0% compared to the standard CLIP zero-shot inference. This is because the additional steps in our pipeline, subtracting a centroid and aggregating predictions, primarily consist of highly optimized vector operations on pre-computed features. This marginal increase in computation demonstrates that SHED is a highly efficient framework, making it practical for deployment in real-world scenarios without significant performance trade-offs.

E.2 Impact of Textual Centering

We conducted an experiment to quantify the benefit of using diverse domain-styled prompts for textual centering. We compare our standard approach against a variant that computes the global text centroid using only a single generic prompt (i.e., “a photo of a {class name}”).

The results in Table 10 show that using diverse domain-styled prompts yields a 0.3% performance gain on the challenging DomainNet benchmark. This confirms that enriching the text modality with varied style cues helps create a more robust and representative global text centroid. This, in turn, mitigates potential biases introduced by a single, generic prompt and contributes to a more effective style-homogenized alignment.

E.3 Ablation on Centroid Update Strategy

In our method, the source domain centroids (μ_s) are computed once before training and remain fixed. We compare this design choice against an alternative strategy where the centroids are updated dynamically during training using an Exponential Moving Average (EMA).

Table 11 shows that using EMA to update centroids during training leads to a significant performance degradation of 11.8% on DomainNet. We attribute this to the instability introduced by dynamically shifting centroids, which can disrupt the delicate process of aligning style-homogenized embeddings, especially in the early stages of training. In contrast, using fixed centroids computed from the powerful pre-trained CLIP encoder provides a stable anchor for style removal, preserving the model’s geometric structure and leading to better generalization.

Method	Clipart	Infograph	Painting	Quickdraw	Real	Sketch	Avg
CLIP Zero-Shot	71.3	47.4	66.4	14.2	83.4	63.1	57.5
CoOp	75.1	49.5	69.6	15.8	81.7	66.8	59.8
CoCoOp	74.8	51.9	69.2	16.0	80.9	67.2	60.0
MIRO	-	-	-	-	-	-	54.0
CLIPood	77.8	54.5	72.6	20.2	85.6	70.1	63.5
CLIPCEIL	-	-	-	-	-	-	63.6
SHED (ours)	78.3 \pm 0.1	55.0 \pm 0.2	72.9 \pm 0.2	21.0 \pm 0.4	85.8 \pm 0.1	70.3 \pm 0.2	63.9 \pm 0.1

Table 8: Comparison of classification accuracy on DomainNet. The best results are in **bold**.

Method	Inference Time (ms/sample)	Overhead
Zero-Shot CLIP	10.0	-
SHED (Ours)	10.8	+8.0%

Table 9: Comparison of inference time and computational overhead. The overhead is calculated relative to the CLIP zero-shot baseline.

Centering Strategy	DomainNet Accuracy (%)
Single Generic Prompt	63.6
Diverse Domain-Styled Prompts	63.9

Table 10: Performance comparison on DomainNet using different textual centering strategies. Our approach utilizes diverse domain-styled prompts.

E.4 Comparison with Tip-Adapter in Zero-Shot Setting

To further situate our contribution, we compared our style-homogenized zero-shot inference mechanism with Tip-Adapter, a strong parameter-efficient fine-tuning method adapted for the zero-shot domain generalization task. For a fair comparison, both methods are applied directly on the pre-trained CLIP model without any training.

As detailed in Table 12, our style-homogenized zero-shot approach outperforms Tip-Adapter by 1.2% on DomainNet. While Tip-Adapter adapts to downstream data using a cached set of features, it does not explicitly account for domain style shifts. Our method, by directly modeling and mitigating style variations through centroid manipulation, proves to be a more effective mechanism for improving zero-shot generalization. This result further validates that explicitly addressing the style information in embeddings is a crucial component of our framework’s success.

F Limitations and Future Work

While SHED demonstrates strong performance, we acknowledge several limitations and avenues for future research. First, our method relies on a pre-defined set of textual domain prompts to construct synthetic centroids during inference. While we show this is robust, performance could potentially be further improved by developing methods to automatically generate or adapt these style prompts based on the test sample itself. Second, the effectiveness of style centering depends on the assumption that a domain’s style bias can be reasonably captured by the centroid of its feature distribution. This

Update Strategy	DomainNet Accuracy (%)
EMA Update	52.1
Fixed Centroids (Ours)	63.9

Table 11: Performance on DomainNet with different centroid update strategies.

Method	DomainNet Accuracy (%)
Tip-Adapter (Zero-Shot DG)	58.8
Style-Homogenized Zero-Shot	60.0

Table 12: Comparison with Tip-Adapter on DomainNet in a zero-shot setting. Our method applies the domain-agnostic centroid aggregation inference on the original CLIP model.

may be less effective for domains with highly multi-modal style distributions. Future work could explore more sophisticated density estimators to model domain styles. Finally, applying and evaluating the SHED framework on other vision-language backbones and extending it to other DG tasks, such as semantic segmentation, represents a promising direction for future investigation.